Chapter 1

Introduction

1.1 Stellar Classification and Evolution

At the heart of every star lies a profound mystery—a dynamic that not only breathes life into stellar magnetic fields but also weaves the intricate patterns of variability that echo across the cosmos. These dynamics affect everything that comes near the vicinity of stars, including planets, their moons, meteors, asteroids, and other stellar objects. In order to identify to what extent these stellar activities affect its vicinity, we need to know at what evolutionary stage they are, and then they can be classified accordingly. Ejnar Hertzsprung and Henry Norris Russell did the classification of stars, which is famously recognized as the Hertzsprung-Russell (H-R) diagram (Hertzsprung, 1908; Russell, 1914), as reproduced in Fig. 1.1. These classifications help astronomers understand stars' physical properties and life cycles by providing a framework to compare and analyze different stars. The spectral classification (OBAFGKM) (Trumpler, 1925, 1930) reveals a star's temperature and color, indicating its surface conditions and energy output. The luminosity class gives insights into a star's size and brightness, which relate to its stage in the life cycle. For instance, main sequence stars are in a stable phase, burning hydrogen in their cores, while giants and supergiants are more evolved, having exhausted their core hydrogen.

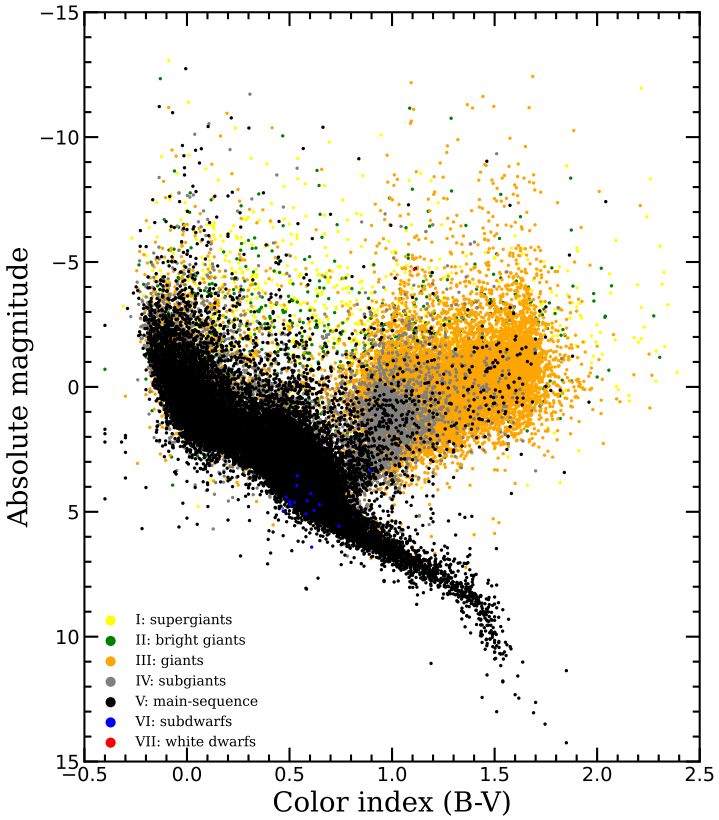

Figure 1.1: HR Diagram reproduced using HIPPARCOS catalog.

By placing stars on the H-R diagram, astronomers can trace their evolutionary paths. For example, a low-mass star like the Sun (spectral type G2V) is currently in the main sequence stage of its life, during which hydrogen is converted into helium through nuclear fusion in its core. Eventually, the Sun will exhaust its hydrogen, and the buildup of inert helium will destabilize the core, causing it to heat up and expand. This will lead the Sun to grow in size and become a red giant. Fortunately, we still have about 5.4 billion years before this dramatic transformation occurs. After this red giant phase, the Sun will ignite helium for several million years before shrinking to about a tenth of its current size, ultimately becoming a white dwarf. In contrast, stars that have mass significantly more than the Sun— usually those with an initial mass exceeding 20 to 25 times that of the Sun are likely to end their life as black holes. Specialized classifications, such as Wolf-Rayet stars and

brown dwarfs, offer insights into the more unusual and extreme stages of stellar evolution. Overall, these classification systems enable astronomers to predict a star's past, present, and future, deepening our understanding of stellar physics and the broader cosmos.

1.2 Stellar Activity: Observation perspective

Our closest star, the Sun, displays a periodic cycle with a duration of 22 years (11 years in strength), characterized by a relatively smooth variation in amplitude over the long term (beyond the 22-year cycle). It also experiences occasional grand minima, which are extended phases of reduced activity (Usoskin, 2017; Biswas et al., 2023). Different stars, in contrast, show a wide range of variability in the magnetic cycles (Baliunas et al., 1995).

While solar observations date back to around 800 BC, the underlying nature of solar magnetic fields remained elusive until 1908. That year, George E. Hale, working at the Mount Wilson Observatory (MWO), made a groundbreaking discovery by analyzing the splitting of spectral lines (commonly known as the Zeeman effect). He determined that sunspots—dark patches on the Sun's surface—are regions of intense magnetic fields (Hale, 1908). These fields typically have strengths of around 10^3 G, but can reach values between 2,000 and 3,700 G. This marked the first observation of a magnetic field beyond Earth.

It was soon realized that the magnetic activity of the Sun differs significantly from that of Earth, which in turn sparked interest in the magnetic activity of other planets and stars. Now, a key question in modern astronomy is understanding how magnetic activity forms and changes in different stars and other objects in space.

In recent years, there has been significant progress in observing late-type stars, which include Sun-like stars with varying masses, rotation rates, convection patterns, and magnetic field strengths. By Sun-like stars, I refer to stars that share properties similar to our Sun, including mass, temperature, and evolutionary stage. Classifying these stars can be complex, but they generally fall into three main categories:

(a) Solar-Type Stars (Solar-like): These stars have similar masses and evolutionary

stages to the Sun. They typically range in spectral classification from F8V to K2V, corresponding to a B−V color index of approximately 0.50 to 1.00. This makes them relatively bright and easier to study compared to other types of stars. A few examples include HD 217014 (51 Pegasi), HD 186427 (16 Cyg B), HD 20781, and HD 10180 (Soderblom & King, 1998).

(b) Solar Analogs: These stars closely resemble the Sun in terms of temperature (5278 to 6278 K) and chemical composition but may vary in age or other characteristics. They serve as important benchmarks for understanding solar phenomena. Some examples of solar analogs include HD 186408 (16 Cyg A), HD 095128, and HD 168009 (Soderblom & King, 1998; Soubiran & Triaud, 2004).

(c) Solar Twins: These stars are nearly identical to the Sun in all significant aspects, including mass, age, and chemical composition. They offer valuable insights into the Sun's past and future by serving as direct comparisons. Some of the solar twins include HD 146233 (18 Scorpii), HD 186408 (16 Cyg A), and HD 19445 (Soderblom & King, 1998; Soubiran & Triaud, 2004).

Although Sun-like stars are similar to our Sun, observations have revealed diverse forms of stellar activity, distinct from what we see in the Sun. This creates a two-way benefit in astrophysics: what we learn from studying the Sun can be applied to these stars, and, in turn, studying these stars under different conditions can enhance our understanding of the Sun's behavior.

One key factor influencing stellar activity is rotation. Skumanich (1972) and Rengarajan (1984) show that the faster a star rotates, the more magnetically active it becomes. In fact, the activity-rotation relationship has already been established by Noyes et al. (1984a) through observations of Ca II H & K emissions and recently and more rigorously by Wright & Drake (2016) using X-ray emissions.

It is well known that the Ca II H and K spectral lines are among the best proxies for measuring solar magnetic activity (Leighton, 1959; Skumanich et al., 1975; Schrijver et al., 1992). These lines can also be an excellent method for measuring the activity cycles of

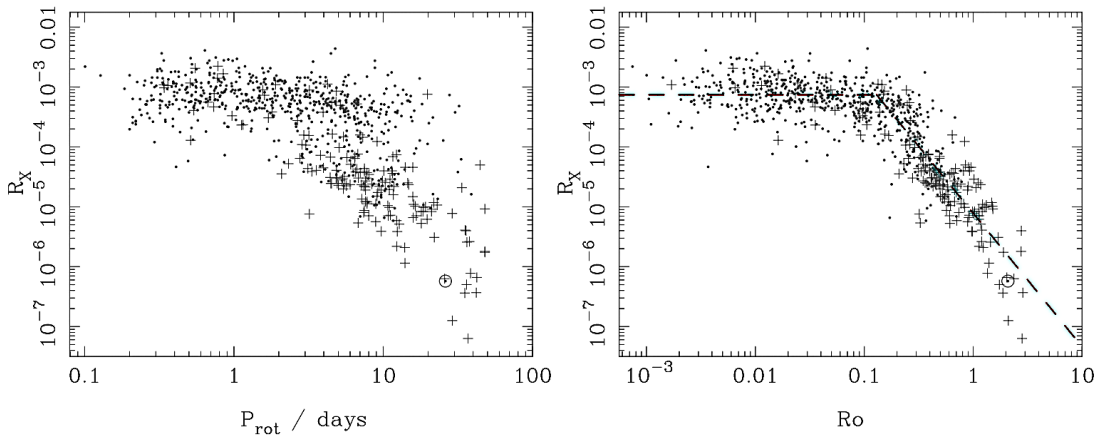

Figure 1.2: Activity-rotation relation in solar-like stars in terms of fractional X-ray luminosity ($R_{\rm X}$) vs. (a) the rotation period, and (b) the Rossby number ($R_{\rm o}$) of solar-type stars. Image credit: Wright et al. (2011).

stars (Bappu & Sivaraman, 1971; Livingston et al., 2007; Priyal et al., 2014; Chatzistergos et al., 2022). Baliunas S. and her group used the chromospheric emission of Ca II H & K lines of many stars with spectral types from early F to M observed since 1966 through the HK Project of Mount Wilson Observatory (MWO) (Baliunas et al., 1995). They observed similar magnetic activity in late-type stars, like our Sun. However, there is a wide range of variety in their activity. According to their survey, stellar magnetic activity is primarily controlled by rotation. But, the relationship between stellar magnetic activity and rotation was initially observed by Skumanich (1972); Rengarajan (1984); Noyes et al. (1984a). They used the chromospheric emission lines to develop a strong correlation between the magnetic activity of a star and the Rossby number, $R_O = (\nu\tau_C)^{-1}$, where ν is the angular velocity of the star and τ_C is the theoretically predicted convective turnover time. Stars with $R_O < 1$ (fast rotators) exhibit strong and irregular activity, while those with $R_O > 1$ (slower rotators) show more regular, cyclic, or even flat-like activity (Mestel & Spruit, 1987; Priest, 2014). This suggests that the behavior of stellar magnetic activity can be modeled as a nonlinear dynamical system, which transitions through various states—constant, periodic, and chaotic—depending on the star's rotation rate (Jennings & Weiss, 1991). Baliunas et al. (1995) conducted a more detailed study of activity trends in such stars, leading to groundbreaking results. They showed that slowly rotating stars (like the Sun) are less active but exhibit more regular cyclic magnetic activity than rapidly

rotating stars, which are highly active and rarely display smooth cyclic behavior. Therefore, rapidly rotating stars are more magnetically active (Skumanich, 1972; Rengarajan, 1984). Using Ca II H & K and X-ray emissions, Noyes et al. (1984a); Wright & Drake (2016) further demonstrated that the activity decreases with the decrease in rotation rate (or increase in rotation period) for slow and moderate rotators, while the magnetic activity saturates for the rapidly rotating stars (with rotation periods of approximately 10 days or less) (as shown in Fig. 1.2). For reference, the fastest-rotating young late-type stars have rotation periods on the order of 0.3 days, while the Sun, a slower rotator, has a rotational period of about 25 days.

The primary reason for this trend can be explained as follows: when stars first enter the main sequence, they are highly active and exhibit a range of rotation speeds. Over time, stellar winds cause these stars to lose angular momentum, slowing their rotation in a process known as magnetic braking. This leads older stars to rotate more slowly. In fact, Skumanich (1972) showed a power-law relation describing the decline in the rotation rate of older main-sequence stars, with their angular velocity decaying as $t^{-1/2}$. This demonstrated a clear link between a star's age and its rotation rate, and thus also between age and magnetic activity, with younger stars generally being the most active. Hence, the primary goal of this thesis is to make detailed dynamo models for the stars of different rotation rates and explain these observational trends of the magnetic activity with rotation rate.

Observations reveal a wide range of magnetic activity in other stars, such as cyclic variations in chromospheric and coronal emissions, starspots, differential rotation, magnetic field structures, and stellar flares. These activities are often much more intense than what we see in the Sun. For example, starspots can be over 100 times larger and cover up to 30% of the star's surface, magnetic flux can be 100 times stronger, and flares can be 1,000 times more energetic.

Understanding the solar dynamo is a key step towards developing comprehensive theories for stellar dynamos. The challenge lies in explaining the extreme activities observed in other stars, as solar activity seems modest in comparison. Determining which physical

parameters and processes are responsible for these differences is crucial for advancing our understanding of stellar magnetism.

1.2.1 Sun vs other stars: from ordinary to extraordinary

Using the characteristics outlined earlier, we can deduce that the Sun is a typical star. HR diagram clearly categorized the Sun as a G-type star, specifically G2V, anchoring it firmly in the lower middle of the main sequence. This placement indicates that the Sun is in the stable, mid-life phase of stellar evolution, characterized by a moderate surface temperature of approximately $5,500^{\circ}$ Kelvin. Its luminosity is neither as high as the larger giants and supergiants nor as low as the white dwarfs and smaller main sequence stars, making its properties quite average within the vast diversity of stars charted on the H-R diagram.

This comparative understanding of the Sun relative to other stars provides crucial context for studying its behavior and properties. Given that the Sun is our nearest star, with documented observations dating back to 1600 AD, studying its magnetic field generation and maintenance offers insights not just into its own life cycle but also provides clues about the past and potential future states of similar stars.

Solar vs stellar observations

1.) Sunspots and Starspots

Around 800 BC, the Chinese observed some “dark spots” on the solar surface (photosphere) with their naked eyes. However, Galileo made detailed drawings of sunspots in 1610 AD and published them in 1613. He observed that sunspots were features on the solar surface. He noted that these spots moved across the Sun’s disk, indicating that they were part of the Sun itself and not small planets or moons orbiting it, as some others initially speculated. While sunspots have been observed for centuries, their underlying nature remained elusive until 1908. George Ellery Hale, working at the Mount Wilson Observatory, made a groundbreaking discovery by analyzing the splitting of spectral lines (known as the Zeeman effect). He determined that sunspots are regions of intense mag-

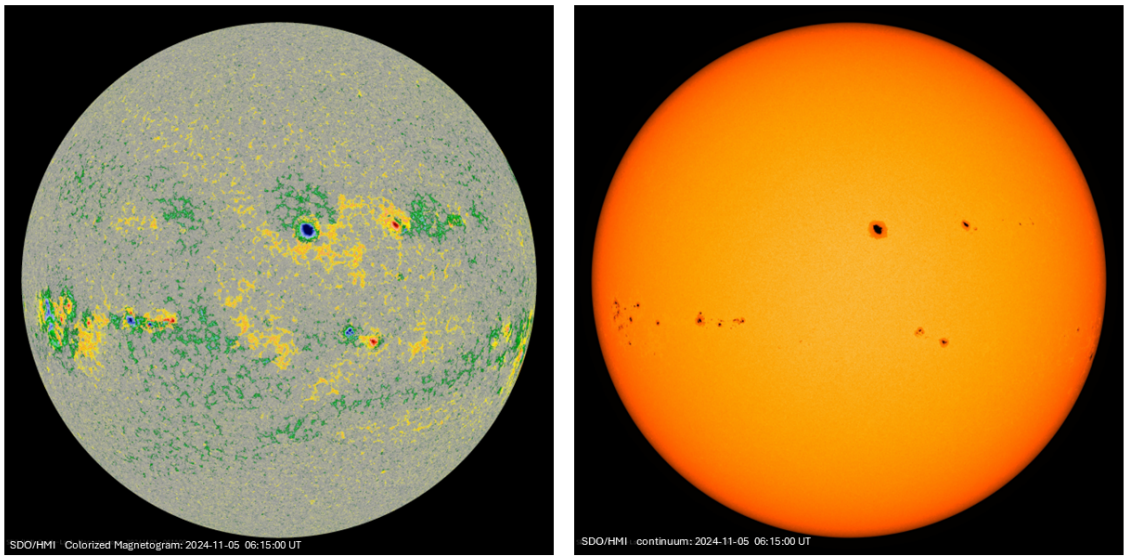

Figure 1.3: Full-disk images of sunspots on the solar surface. The left image is a colorized magnetogram of the Sun (at 6173 Å spectral line of Fe I with a color table ranging from -1500 G to 1500 G. Fields weaker than 24 G are shown in grey, while green and blue represent positive fields, and yellow and red indicate negative fields), highlighting the magnetic activity of the sunspots visible in the white-light image (intensity continuum) on the right. Image credit: NASA: SDO/HMI.

netic fields. These fields, typically around 10^3 G, can reach strengths of up to 2000-3500 G. This marked the first observation of a magnetic field beyond Earth. The strong magnetic fields in sunspots inhibit convection in those areas, leading to inefficient heat transfer to the photosphere. This reduced heat supply causes the temperature in sunspots to drop to around 3000-4000 Kelvin, compared to the surrounding areas, which measure about 5500 Kelvin. Consequently, this temperature disparity makes sunspots appear darker in the visible spectrum. Sunspots, observed in white light, vary significantly in shape, size (disk area), and lifespan, exhibiting a broad spectrum of characteristics. A typical sunspot has a radius varying from 3.5-60 Mm and is formed with two regions: the central dark region is the umbra, and the outer lighter part around it is the penumbra; its flux is about 10^{22} Mx, forms within 30° latitude and have a life span varying from a few hrs to more than a week (Thomas & Weiss, 2008). Sunspots often appear in pairs, representing regions of opposite magnetic polarity located near each other. Each sunspot pair is called a Bipolar Magnetic Region (BMR), with leading and trailing polarities as the two opposite magnetic polarities. The line connecting the centers of the leading and trailing polarities in a BMR

forms an angle with the solar equatorial plane, known as the tilt angle (δ) of the respective BMR. The average till angle for the Sun is about $8°$. The orientation of all BMRs in one hemisphere is opposite to the BMRs in another hemisphere (Hale et al., 1919). Identifying and tracking BMRs to study their long-term evolution remains a popular research interest. Several catalogs exist for observed active regions (ARs)/BMRs, including the NOAA AR catalog, SHARP (Bobra et al., 2014), AutoTAB catalog (Sreedevi et al., 2023), and many others.

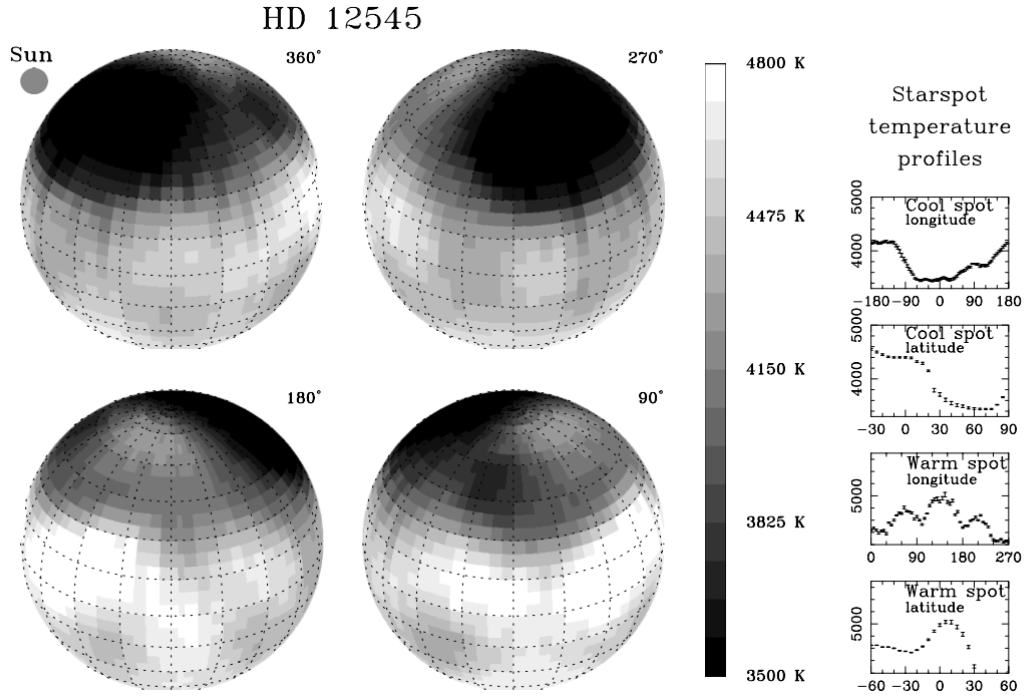

Figure 1.4: Spherical projection of the average temperature map of the K0 III star, XX Trianguli (HD 12545), illustrating the starspots. The size of the solar disk is included on the upper left for comparison. On the right, small panels present temperature profiles along both longitudinal and latitudinal cuts through the warm and cool spots. Image Credit: Strassmeier et al. (1999)

Like sunspots, starspots are common features on the surfaces of stars and are indicators of stellar activity, yet we still do not fully understand the physical processes that control their formation and duration. Long-term Photometric observations of star brightness variations reveal another similarity: the lifetimes of starspots, like those of sunspots, are proportional to their sizes (Berdyugina, 2005), a relationship established for the Sun (Gnevyshev, 1938; Waldmeier, 1955; Petrovay & van Driel-Gesztelyi, 1997). Furthermore, unlike sunspots, observations indicate that some stars develop very large and long-lasting spots in their

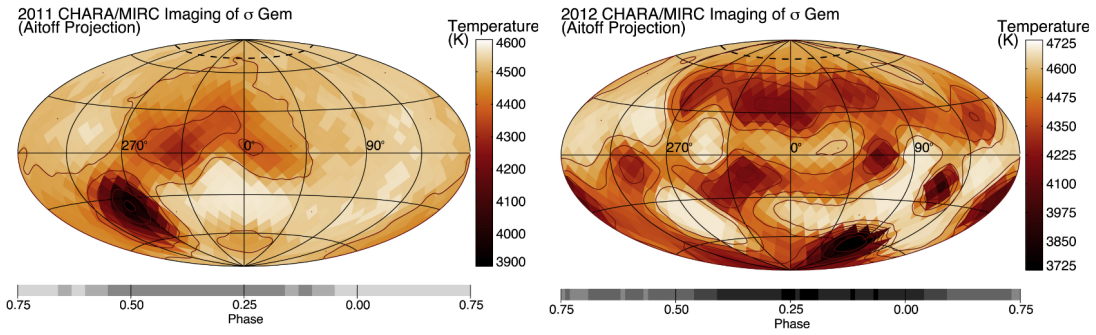

Figure 1.5: Starspots identified using the interferometric map of a K-giant σ Geminorum from 2011 (left) and 2012 (right), Image credit: Roettenbacher et al. (2017)

polar regions (Strassmeier et al., 1999). For example, sunspots can last from a few days to a month, covering a few percent of the solar surface, while spots on certain pre-main-sequence stars, like T-Tauri and K giant star XX Trianguli (as shown in Fig. 1.4), can be as large as 20% of the star's surface and persist for several years (Hall & Henry, 1994; Strassmeier et al., 1999). Another example of a starspot is shown in Fig. 1.5, which depicts the K-type giant star σ Geminorum. Roettenbacher et al. (2017) observed large spots on σ Geminorum using interferometric, spectroscopic, and photometric data. Another comparison between sunspots and starspots is that young and hotter stars show a greater contrast in brightness between spot regions and the surrounding photospheric surface, indicating that the temperature difference between these areas increases with stellar temperature. For instance, stars of spectral type G0 have a temperature difference of about 2000 K, whereas in stars of type M4, this difference is only around 200 K. This characteristic is observed in both active dwarf and giant stars, with cooler dwarfs generally having stronger magnetic fields that cover larger areas (Berdyugina, 2005). Therefore, in the past few decades, advancements in observational tools and diagnostic techniques have greatly enhanced our understanding of starspots and stellar activity.

2.) Solar and Stellar cycle

The careful observations of these dark spots on the solar surface reveal that their number and size vary with time and usually peak every 11 years. This periodic variation of the number of sunspot/sunspot areas is called the solar cycle or sunspot cycle. This cycle

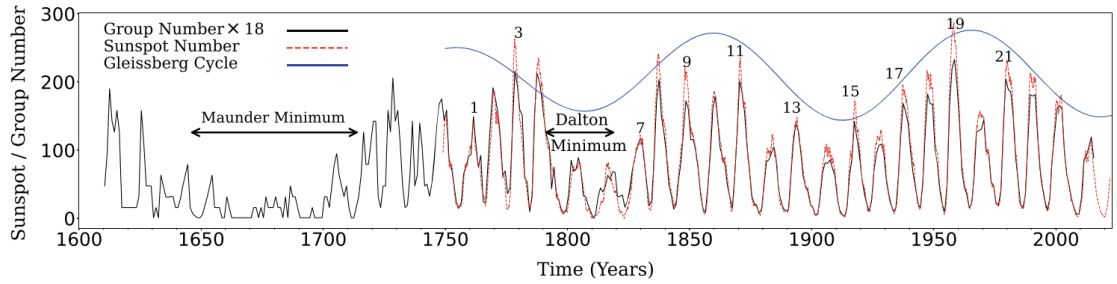

Figure 1.6: Solar cycle: Variation of the number of sunspot (red dotted curve)/sunspot areas/sunspot group number(black curve). Image credit: Karak (2023a).

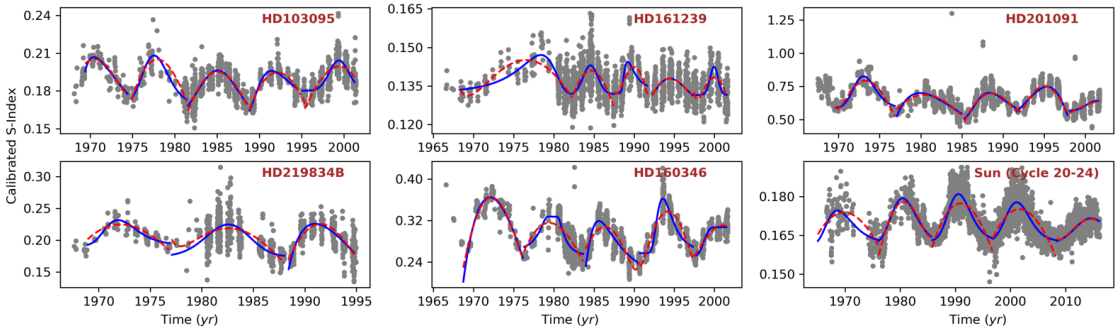

Figure 1.7: Representation of a few good cycles from old to intermediate stars of spectral type G and K as measured by the MWO-calibrated Ca II emission fluxes (S-index). Red and blue curves are the fitted profiles given in Garg et al. (2019)

typically spans about 11 years from one solar minimum to the next, though the length can vary from 9 to 14 years. For each cycle, the Sun's magnetic field completely flips, with the north and south poles switching places. Along with this, other solar activities, such as solar flares and coronal mass ejections, also increase and decrease during the solar cycle.

As for now, The international sunspot number (ISN) is widely regarded as one of the most reliable proxies for solar activity due to its long-term availability. A few others, such as sunspot area, 10.7 cm Solar Flux (Tapping and Charrois 1994), etc., have also been regularly used for the same. Fig. 1.6 shows the temporal variation of daily sunspot area.

However, observing starspots is more challenging than observing sunspots because of how far they are. As a result, counting starspots on a daily or monthly basis has been difficult, highlighting the need for an alternative stellar activity proxy. One such solar proxy is the Ca II H and K lines, which is among the most effective indicators of the solar magnetic field. Over the past few decades, the magnetic fields of stars have been measured by monitoring the Ca H and K emission cores (chromospheric emission), which is known to

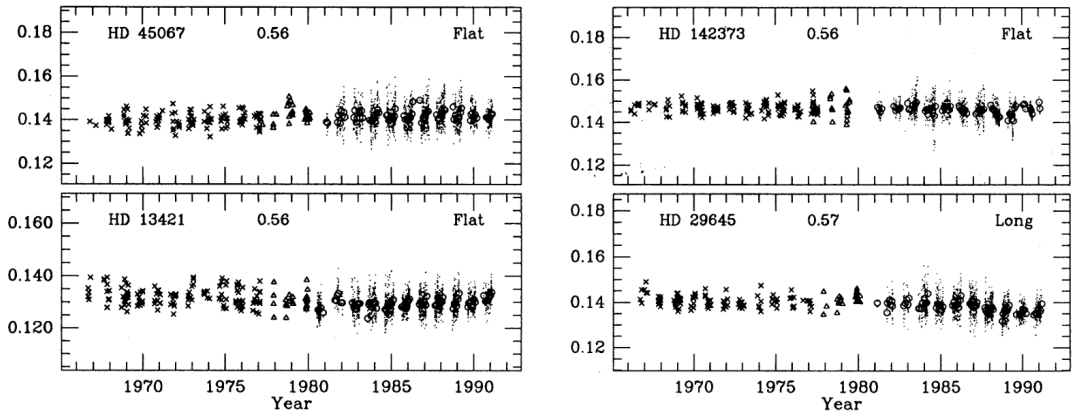

Figure 1.8: A few examples of stellar cycles of old stars depicting flat-like activity as identified by Baliunas et al. (1995). Vertical axis shows the Ca II emission in S-index unit.

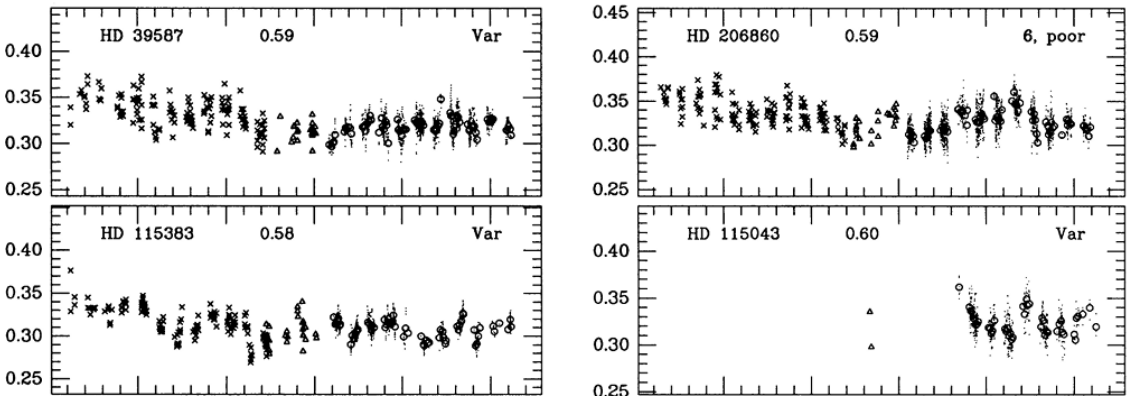

Figure 1.9: Same as Fig. 1.8 but for some stars which show irregular cycles as identified by Baliunas et al. (1995).

be highly correlated with the magnetic field. The S-index derived from Ca H and K data of six different stars, including our sun, is shown in Fig. 1.7. As evident from this figure, different stars show different types of cycles and all these cycles are irregular.

However, I would be biased to highlight only the five stars with nice, regular cycles like our sun. Fig. 1.7 shows only old-intermediate aged stars with regular cyclic behavior and represent 'good' cycles. After analyzing the data of about 111 Sun-like stars, Baliunas et al. (1995) classified stars based on their age, spectral type, and cyclic behavior. To simplify, I have grouped these into what I like to call the "good," "bad," and "ugly" cycles.

Fig. 1.7 shows only older stars with regular cyclic behavior, which I consider as "good" cycles. In addition, some stars show flat activity, remaining in a constant minimum phase, I consider them as "bad" cycles. Some examples of such stellar cycles are shown in Fig. 1.8. One reason for this flat activity could be that these stars are in a Maunder-minimum phase and may develop cyclic behavior in the future. To support this hypothesis, one such star, HD 23249 ($\delta\ \epsilon ri$), previously exhibited flat activity according to Baliunas et al. (1995) but later began displaying cyclic behavior. The last category includes stars with very irregular activity. Baliunas et al. (1995) speculated that these are young stars, and I refer to them as "ugly" cycles. Some examples of irregular stellar cycles are shown in Fig. 1.9. In summary, the younger stars, in general, rotate rapidly and exhibit stronger magnetic fields with irregular cycles, while the older stars, like our Sun, rotate slowly and have weaker magnetic fields, with fairly regular cycles with occasional Maunder minimum-like events.

Hence, a few of the questions I shall address in my thesis include:

- Why are the stellar cycles not regular?
- Which parameters of the star determine the amount of variability in the stellar cycle?
- Why do young, rapidly rotating stars show more variability and older, slowly rotating stars show fairly regular cycles?
- Why do not all stars show Maunder minimum-like extended episodes of weaker magnetic activity?

- Can we constrain the physics of the origin of the solar magnetic field better by modelling the magnetic cycles of other stars?
- How do the dynamo mechanism in rapidly rotating stars differ from the of slowly rotating stars?

Characteristics of the solar and stellar cycles

The consistent extended observations of the sunspots over numerous years and cycles has uncovered a lot of its characteristics. A few of these are mentioned below:

(a) Butterfly Diagram

It is a graphical representation that illustrates the latitudinal variation of sunspot activity over a solar cycle. It is named after its shape, which resembles a butterfly with outstretched wings. From this figure, we can see that, at the beginning of the cycle, the sunspots appear in the mid-latitudes ($30° - 40°$) in both hemispheres, whereas with the progression of the cycle, sunspots shift progressively toward the equatorial region.

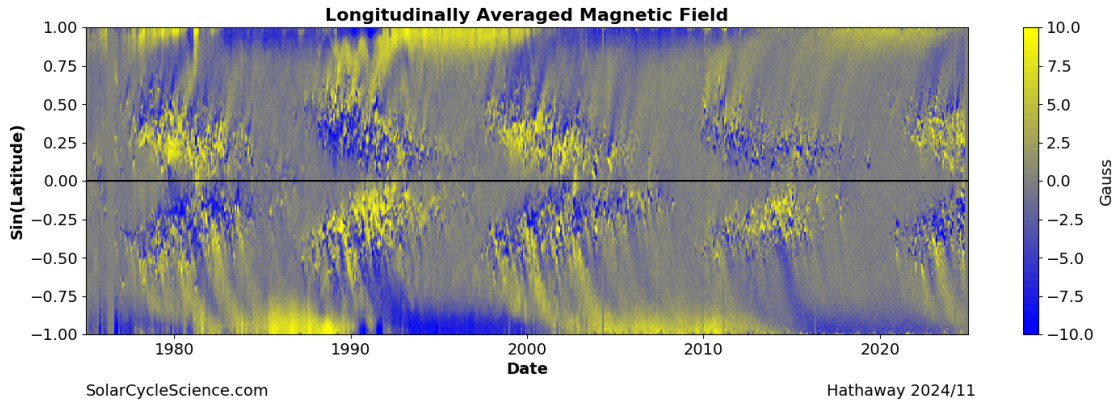

Figure 1.10: Magnetic butterfly diagram: Longitudinally averaged distribution of the surface radial field over the past four solar cycles, obtained from instruments on Kitt Peak, SOHO and SDO. Image credit: Dr. David H. Hathaway via www.solarcyclescience.com

Since this is a fundamental feature of the solar cycle, we also expect to see a butterfly-like diagram in stellar cycles. However, once again, observational constraints make this challenging. Despite these limitations, Bazot (2018) derived the first stellar

butterfly diagram in HD 173701 (a solar analog star), by combining information from asteroseismic and photometric analyses.

(b) Cycle period vs rotation period dependence

The period of the solar cycle, like any other periodic function, is defined as the interval between two successive minima, typically encompassing a maximum or sometimes multiple maxima. Despite being periodic, solar cycle does not seem to be regular; the strength, amplitude, and length vary from cycle to cycle. Also, each cycle tends to begin slightly before its preceding minimum and extend a bit beyond the subsequent maximum. Therefore, it is a bit challenging to determine the cycle period. Generally, the average cycle period is computed by dividing the time span between two minima by the number of cycles covered. This method yields an average cycle duration of approximately 131.7 months (about 11 years), according to Hathaway (2015). We can also determine the cycle period using the power spectra analysis, which gives the cycle period to be 132 months (about 11 years).

The cycle period is a characteristic feature of stellar cycles. Given that different stars display various cyclic behaviors, their cycle periods also differ. Most of the early observations predominantly concentrated on the activity-rotation relationship in Sun-like stars, with some studies identifying a correlation between cycle period and rotation period (Noyes et al., 1984b; Soon et al., 1994). Using chromospheric activity data from Mount Wilson Observatory (MWO) and HARPS (High Accuracy Radial Velocity Planet Searcher) for 4,454 cool stars, Boro Saikia et al. (2018) revealed that the relationship between cycle period and rotation period is different for fast and slowly-rotating stars. As illustrated in Fig. 1.11, for rapidly rotating stars, the cycle period somewhat tends to decrease as the rotation period increases, whereas, for slow rotators, the cycle period tends to increase with the rotation periods. However, this trend is quite complicated for fast-rotating stars.

(c) Grand Minima and Maxima

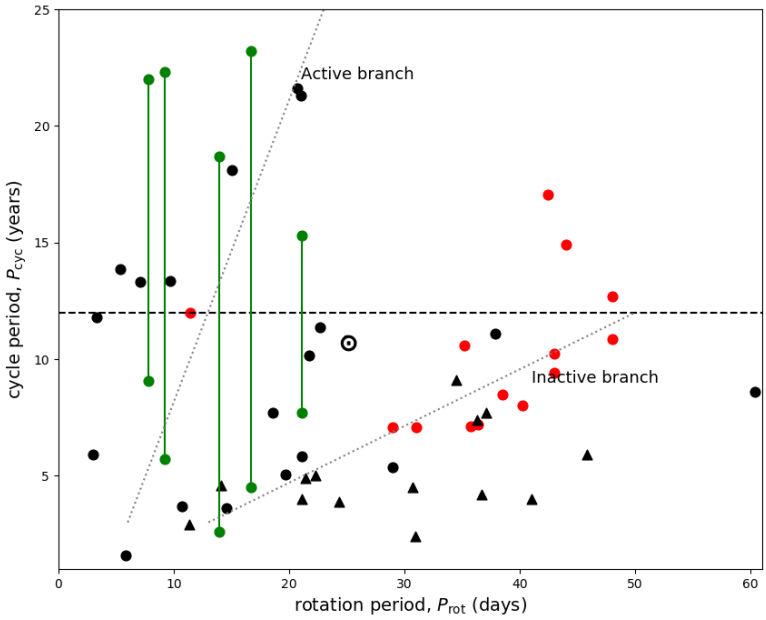

Figure 1.11: Cycle period vs rotation period: Red, green, and black symbols represent stars with well-defined cycles, multiple or chaotic cycles, and unconfirmed cycles, respectively, based on data from Mount Wilson (solid circles) and HARPS (solid triangles). Vertical green lines connect the two cycle periods of a star exhibiting dual cycles. The dotted lines depict the active and inactive branches of stellar activity cycles, as described by Böhm-Vitense (2007). Sun is marked as ⊙. Image credit: Boro Saikia et al. (2018).

While observing the long-term variation of the solar cycle, we do realize that the amplitude and strength of the solar cycle vary a lot. In fact, sometimes solar activity is significantly reduced for an extended period, resulting in fewer sunspots and lessened solar phenomena compared to typical solar cycles. These episodes can last for decades or even longer and are of great interest to scientists because of their impact on space weather and Earth's climate. One of these events is called the "Maunder Minima" which occurred during the 17th century when unusually low sunspot activity was seen with less or no sunspots, which lasted for about 70 years (Eddy, 1976). This period coincided with a time of ice-age on Earth, leading to the hypothesis that solar activity might influence climate. Many other proxies of the solar activity cycle, such as Carbon-14 and Beryllium-10, also reveal similar results of weak activity during those periods. These observations have the last 11,000 years of sunspot data. According to Usoskin et al. (2007); Usoskin (2013), the Sun has

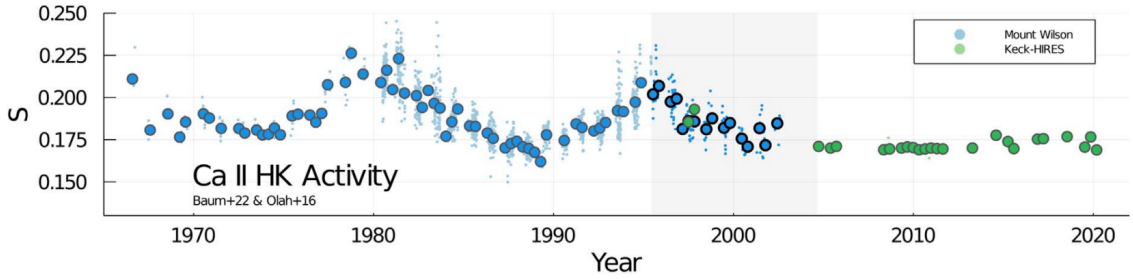

Figure 1.12: S-index time series for K2V star, HD 166620 showing entering into Maunder minimum phase. Blue points depict data from Mount Wilson, and green points show from the Keck HIRES. Image Credit: Baum et al. (2022)

observed 27 such events of reduced magnetic activity, and it will continue to have them in the future. One such event is also marked in the Fig. 1.6.

Different stars, in contrast, show a wide range of variability in the magnetic cycles. Baliunas et al. (1995) noted that old-slowly rotating stars display smoother variability along with occasional grand minima in their magnetic activity cycles. Conversely, they found that fast-rotating young stars exhibit highly irregular activity and do not show any grand minima. Similar findings were reported by Oláh et al. (2016); Boro Saikia et al. (2018); Garg et al. (2019), who used additional data to support these observations. More recently, Baum et al. (2022) revealed that a K2V star, HD 166620, has entered into a grand minimum phase. Flores Trivigno, M. et al. (2024) also suggested that HD 217014 and HD 20807 are possibly Maunder minimum candidates. An important point here is that all of these potential Maunder minimum candidates are slow-rotating stars. However, no studies have yet explored the relationship between the occurrence of Maunder minima and a star's rotation rate. In this thesis, we will also make efforts to investigate the connection between Maunder minima occurrences and stellar rotation rates.

(d) Waldemeir effect

It suggests that the rise time of a solar cycle is less than the time it takes to reach from maximum to minimum (Waldmeier, 1935). Furthermore, the rise time of a cycle is anti-correlated with the amplitude of the next cycle (Waldmeier, 1935, 1939). The theoretical explanation for the observed effect was given by Karak & Choudhuri

(2011). Some stellar cycles (e.g., HD 10476, HD 16160) are remarkably similar to the solar cycle in a way that they exhibit many of the same cyclic features we observe in the Sun. The Waldmeier effect is one such feature that many stars display (Garg et al., 2019).

1.2.2 Large-scale flows in Sun-like stars

The movement of the starspots across the stellar surface can explain a lot about the flow properties on its surface. These flows play a crucial role in the stellar magnetic activity and the stellar dynamo, which generate and sustain the magnetic field in stars. The essential large-scale flows in any star include differential rotation and meridional circulation. This section will describe these observations.

Solar Differential Rotation

Just like Earth, the Sun also rotates along its axis. However, unlike Earth's surface, its rotation is not like that of a solid body; it rotates differentially. Each latitude rotates at a different speed. The equator rotates faster than its poles by 30%, a phenomenon known as differential rotation. As seen from Earth, the equatorial regions complete a rotation approximately every 25 days, while the polar regions take about 35 days to complete one rotation. Historical observations of sunspots and other solar features have frequently been used as tracers to measure the differential rotation of the Sun's photosphere. The study of solar rotation has a rich history of observations. Christoph Scheiner, in 1630, first identified variations in rotation periods across different latitudes by tracking sunspot movements (Paternò, 2010). In the modern era, the Doppler effect is employed to measure the rotation rate (e.g., Howard & Harvey, 1970). However, a significant advancement in understanding solar differential rotation was achieved with the advent of helioseismology. Helioseismology utilizes acoustic waves to understand the Sun's internal structure and has allowed for the measurement of the internal profile of differential rotation (Schou et al., 1998). It says that the differential rotation is not uniform but varies with depth, indicating that different layers of the Sun's interior contribute differently to the overall rotational

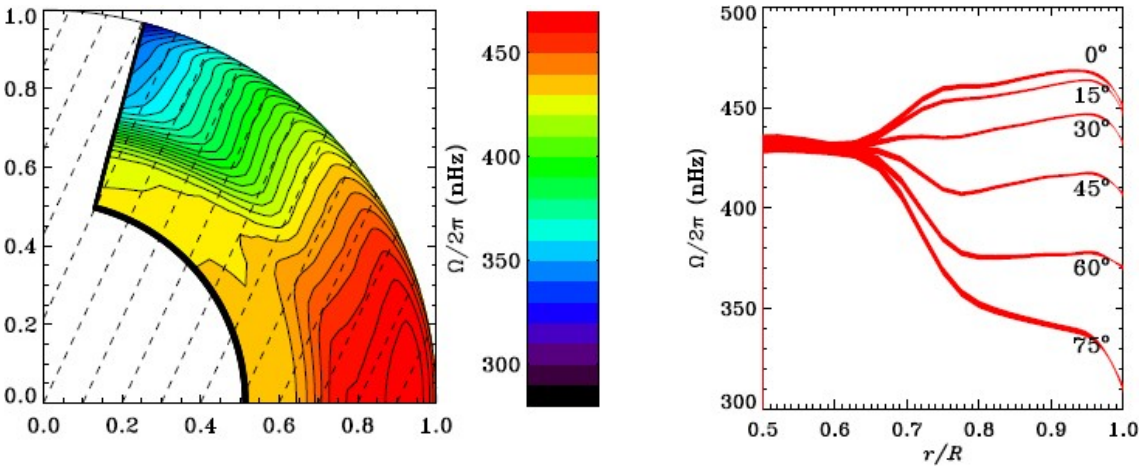

Figure 1.13: Solar differential rotation (left) and rotation profiles at constant latitudes as a function of radius (right), obtained from the global helioseismic analyses. Image credit: GONG data, Howe (2009).

profile. It also allows us to observe the near-surface shear layer and the tachocline at the base of the convection zone.

Now, one may ask, what can be the generational mechanism of the solar differential rotation? The answer lies in the critical understating of the interaction of the rotation on thermal convection in the solar interior. At the core of the Sun, nuclear fusion produces thermal energy. This energy is carried outward by radiation through the radiation zone ($<$ 0.71 R_s, where R_s denotes the solar radius). In the outer region (beyond $0.71R_s$, known as the convection zone), increased opacity makes radiation transport less efficient, leading to energy transport via thermal convection. Due to the high Reynolds numbers, this convection is turbulent. The turbulence, affected by the Coriolis force, becomes anisotropic. This anisotropic turbulence facilitates the transport of angular momentum and contributes to the development of large-scale flows (Lebedinsky, 1941). An example of a solar differential rotation profile observed using helioseismic data is shown in Fig. 1.13. Given the highly nonlinear and chaotic nature of turbulence in the convection zone, numerical simulations are crucial for studying and understanding solar differential rotation.

Stellar Differential Rotation

With advancements in helioseismology, we now have a good understanding of solar differential rotation in the whole convection zone. However, studying differential rotation in

distant stars is much more challenging. The best we can do is observe the nature of their surface flows, which provide clues about their internal structure and dynamics.

One of the most extensive studies of stellar differential rotation was conducted by Hall (1991). This study used long-term light curve data to measure the rotation periods of stars. Differences in these periods were interpreted as starspots forming at different latitudes, indicating differential rotation. Hall found that the ”lap-time” (the time it takes for the equator to overtake the poles) is nearly the same for stars, regardless of their rotation speed. In other words, the difference in angular velocity between the equator and poles ($\Delta\Omega$) does not vary much between stars, meaning fast-rotating stars behave more like rigid bodies compared to stars like the Sun. Another study by Donahue et al. (1996), using chromospheric emission data, reached a similar conclusion, finding that $\Delta\Omega$ depends only weakly on the rotation rate. Information about the rotation of late-type stars has also been gathered using observations of radial velocity measurements, photometric variability, and asteroseismology (the study of stellar oscillations).

The effects of rotation on stellar oscillation measurements are visible because latitudinal and radial differential rotation can leave signatures on the fine structure of stellar oscillation power spectra. Asteroseismology has advanced enough to probe the interiors of some evolved stars, like red giants and subgiants, but studying Sun-like stars is more difficult due to their slow rotation. The rotational splitting frequencies are often too small compared to the mode linewidths (Aerts et al., 2010; García & Ballot, 2019). In a few cases, clues about angular velocity and rotation axis inclination have been obtained. Some solar-type stars have shown strong latitudinal differential rotation, with the equator rotating faster than the poles (Benomar et al., 2018). The difference in angular velocity between the equator and poles ($\Delta\Omega$) may depend on the average rotation rate of stars, with most of the stars in Benomar et al. (2018)’s study rotating faster than the Sun. For Sun-like stars, only upper limits have been established for radial differential rotation (Nielsen, M. B. et al., 2014). For the stars rotate slower than the sun, the magnetorotational evolution is still not clear. Different studies have reported varying findings: some observers have found certain evolved solar-like stars that follow Skumanich’s law (Lorenzo-Oliveira et al., 2018, 2019),

while others have not (van Saders et al., 2016, 2019; Hall et al., 2021). In addition to this, it is challenging to detect the surface magnetic field evolution in stars rotating slower than the sun. Some theoreticians propose that there might be a chance of observing anti-solar differential rotation, in which poles rotate faster than the equator. Notable candidates for stars showing anti-solar differential rotation include KIC 10907436, KIC 7189915, and KIC 12117868. Therefore, to better understand stellar differential rotation, it is crucial to examine how it relates to factors such as the star's average rotation rate (Ω_*), mass, age, and composition.

Photometric variability caused by starspots and faculae can also reveal details about surface rotation and differential rotation. Information about latitudinal differential rotation can be inferred when these active regions cover a range of latitudes on the stellar surface. Various studies have described the relation between differential rotation and mean rotation rate using a power law ($\Delta\Omega = \Omega_*^m$), although values of the exponent m differ depending on the method and stellar type (Barnes et al., 2005). Fast main-sequence stars, particularly cooler stars, tend to follow this power law more consistently.

Some studies have also explored the effects of stellar composition, such as metallicity, on differential rotation. Stars with higher metallicity, like the solar analog HD 173701, have shown solar-like rotation patterns but with stronger latitudinal contrasts and shorter magnetic cycles (Karoff et al., 2018). However, the sensitivity of the current techniques makes it particularly difficult to observe slow rotators.

In conclusion, differential rotation is a crucial parameter of stellar convective envelopes. Measuring surface rotational contrast in stars, apart from the Sun, remains challenging due to the need for highly precise instruments and long observation periods. The upcoming PLATO mission is expected to bring significant progress in this area (Rauer et al., 2014). Until then, theoretical modeling of these flows remains essential to support ongoing observations and guide future research.

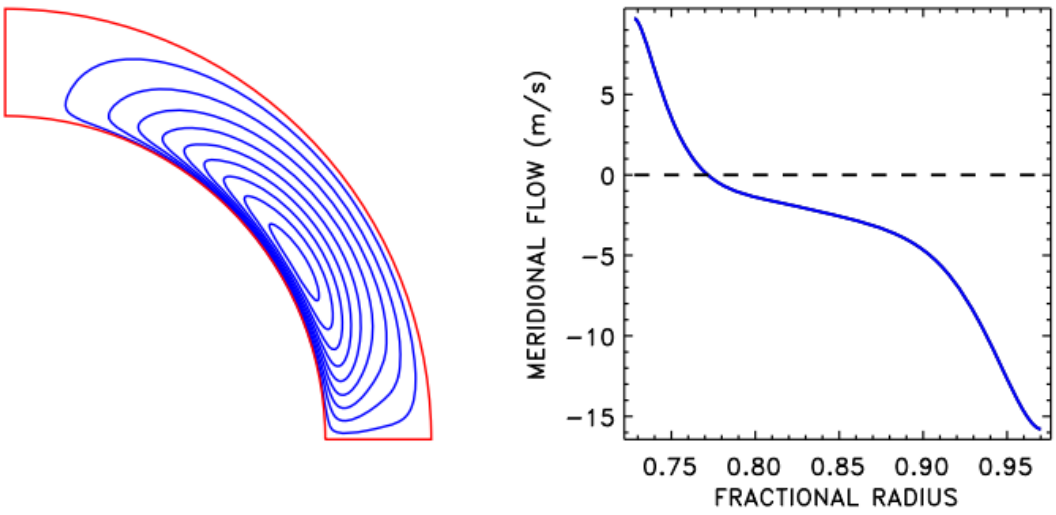

Figure 1.14: Solar meridinal circulation streamlines (left) and its variation with depth ate $45°$ latitude (right). This image is obtained from hydrodynamic mean-field model of Kitchatinov & Olemskoy (2011b).

Meridional Circulations

After differential rotation, the second crucial axisymmetric flow inside the solar convection zone (CZ) is the meridional circulation, which occurs in the meridional plane and is a weak flow of plasma from equator to pole in the upper CZ and from pole to equator in the deeper CZ (Kitchatinov, 2016; Hanasoge, 2022). This flow has been observed on the surface for many years by tracking various tracers.

Even though the flow is very weak, helioseismology techniques can be used to determine the subsurface distribution of the meridional flow. Giles et al. (1997) found that the observed surface flow is approximately constant throughout the outer layers of the Sun (4% of the solar radius). Braun & Fan (1998) confirmed this by showing that the poleward flow extends through the upper half of the convection zone, with no indication of a returning (equatorward) flow in that region. However, this does not rule out the possibility of an equatorward return flow in the deeper layers of the convection zone, though compressibility effects suggest that such a flow would likely be very weak (Gizon et al., 2020). Since meridional circulation is significantly weaker compared to other surface motions, it is challenging to measure accurately. However, it has an interesting property: it carries various solar features towards the poles, allowing for some inferences. For instance, the magnetic butterfly diagram (as shown in Fig. 1.10) reveals the poleward movement of magnetic

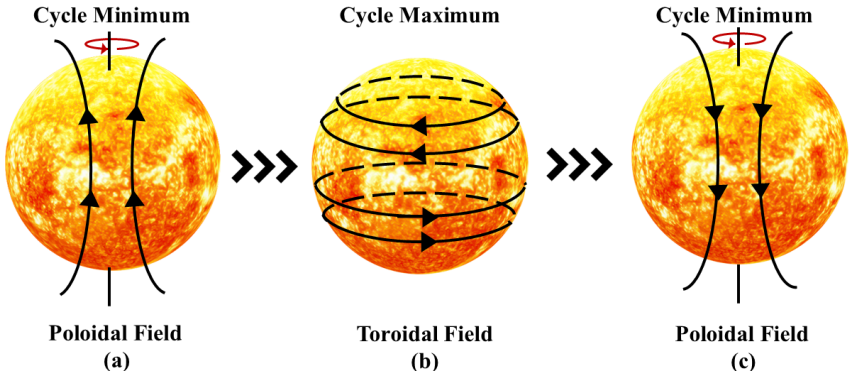

Figure 1.15: Pictorial illustration of cyclic variation of stellar magnetic field as per observations.

flux, which is associated with the reversal of solar polarity. This transport is thought to be facilitated by meridional circulation (Charbonneau, 2010; Choudhuri, 2021a).

Hence, meridional circulation is another crucial parameter of stellar convective envelopes, and its measurements in stars, apart from the Sun, remain challenging due to the unavailability of highly precise instruments and long observation periods. Therefore, theoretical modeling remains essential here to support ongoing observations and guide future research.

1.3 Solar/Stellar Dynamo: A theoretical perspective on observational data

Until now, we have discussed observations related to solar and stellar magnetism, activity cycles, and large-scale flows. Let us now delve into the underlying causes of these observed features of the stellar magnetic field and cycles, drawing on our current understanding of the solar and stellar dynamos, which is believed to operate through the convective motion of ionized plasma within the stellar convection zones.

1.3.1 Dynamo theory

A star's large-scale magnetic field is typically divided into two components: the poloidal and the toroidal fields (as depicted in Fig. 1.15). The poloidal field is characterized by field

lines that connect the stellar poles, while the toroidal field has lines that wrap around the Star's equatorial plane. In a spherical coordinate system centered on a star, the azimuthal (ϕ) component represents the toroidal field (B_ϕ). In contrast, the poloidal field ($B_{\rm P}$) comprises both the radial (r) and co-latitudinal (θ) components. However, this description applies specifically to axisymmetric magnetic fields; for non-axisymmetric fields, the radial (r) and co-latitudinal (θ) components can also contribute to the toroidal field. In the case of the Sun, it is well established that the solar cycle mentioned earlier corresponds to the periodic oscillations of the toroidal and poloidal magnetic fields. At the minimum of a solar cycle, the magnetic field's orientation is predominantly poloidal, while during the maximum, the toroidal component dominates the global magnetic field. The magnetic field's polarity in the polar regions of a hemisphere flips with each successive cycle minimum. This flip is significant because the poloidal field, generated in one cycle, lays the groundwork for the toroidal field of the next cycle. As the poloidal field evolves, the orientation of the leading and trailing of the Bipolar Magnetic Regions (BMRs) also changes with each cycle. These sunspots display distinct polarities that reflect the variations in the underlying magnetic field. This magnetic cycle has an approximate duration of 22 years, during which these polarity reversals occur. Although observational evidences for other stars are limited, we know that stars similar to the Sun have convective cells in their outer layers. Therefore, it is reasonable to expect that a similar dynamo mechanism observed in the Sun operates in other stars, especially Sun-like stars with convection zones in their outer layers.

The solar/stellar dynamo essentially refers to the process that enables the transformation of the poloidal field into the toroidal field and then back from the toroidal to the poloidal one. For the Sun, this process occurs over a timescale of approximately 11 years, corresponding to one complete solar cycle. This dynamo mechanism has been continuous and drives the cyclic magnetic variations observed in stars, such as the butterfly diagram and sunspot activity, as illustrated in the Fig. 1.6.

The current theoretical study of the solar/stellar dynamo primarily focuses on developing numerical models based on existing theories and their associated equations. However,

accurately creating a model that explains all observational aspects of solar/stellar magnetism poses significant challenges due to the limitations of current computational power and algorithms.

To comprehend these numerical models, it is essential to first discuss the foundational principles behind them: magnetohydrodynamics (MHD). MHD is a model that describes the behavior of electrically conducting fluids, such as ionized plasma, in the presence of magnetic field. It provides the framework needed to investigate the physical processes occurring within the ionized plasma of the stellar convection zone, shedding light on the complex dynamics of solar/stellar magnetism. Therefore, let us briefly discuss the fundamental equations of MHD, which is the heart of solar/stellar dynamo models.

Magnetohydrodynamics: The driving force of the Solar/Stellar Dynamo

MHD is a model for understanding the behavior of electrically conducting fluids, such as plasmas, in the presence of magnetic fields. In the context of MHD, plasma is considered as a single fluid. For the effective application of MHD, the length scales of the system must exceed the Debye length, and the time scales should be larger than the inverse of the plasma frequency. Additionally, it is important to apply the nonrelativistic approximation when analyzing plasma dynamics with MHD. These assumptions enable MHD to accurately capture the behavior of plasma in the convection zones of the Sun and other stars. MHD is governed by a set of four equations that combine the Navier-Stokes equations (for fluid dynamics) and Maxwell's equations (for electromagnetism) to describe the complete dynamics of the magnetized system (Choudhuri, 1998). These four equations are presented below, and each term has its standard meaning (refer Priest, 2014, for more details about the given equations).

$$\frac{d\boldsymbol{\rho}}{dt} + \boldsymbol{\rho}\nabla.\mathbf{V} = 0 \tag{1.1}$$

$$\boldsymbol{\rho}\frac{d\mathbf{V}}{dt} = -\nabla p + \frac{1}{\boldsymbol{\rho}}\left(\nabla \times \boldsymbol{B}\right) \times \boldsymbol{B} + \mathbf{F} + \nu\nabla^2\mathbf{V} \tag{1.2}$$

$$\frac{\boldsymbol{\rho}^\gamma}{\gamma - 1}\frac{d}{dt}\frac{p}{p^\gamma} = -\nabla.\mathbf{q} - L_r + \frac{j^2}{\sigma} + F_\mu \tag{1.3}$$

In these equations, $\mathbf{V}$ is the plasma velocity, $\boldsymbol{B}$ is the magnetic field, $\boldsymbol{\rho}$ is the charge density, j is the current density, p is the magnetic pressure and $\mathbf{F}$ is resultant body force, which consists of the gravitational force ($\mathbf{F_g}$) and the viscous force ($\mathbf{F}_\mu = \nu\nabla^2\mathbf{v}$). For incompressible fluid, the continuity equation and energy equation become irrelevant. Ultimately, the most important equation in MHD is the following induction equation. This equation describes how the magnetic field evolves over time in plasma due to the effects of flow and diffusion.

$$\frac{\partial \boldsymbol{B}}{\partial t} = \nabla \times (\mathbf{V} \times \boldsymbol{B} - \lambda \nabla \times \boldsymbol{B}), \tag{1.4}$$

It consists of two main components: the inductive term and the dissipative term. The inductive term represents the source, while the dissipative term accounts for ohmic dissipation. To understand the significance of these terms, we examine their ratio. If V is the velocity, B is the magnetic field, λ is the magnetic diffusivity, and L is the length scale, the ratio of these terms leads to a well-known dimensionless number called the magnetic Reynolds number: $R_\mathrm{m} = \frac{VB/L}{\lambda B/L^2} = \frac{VL}{\lambda}$. Interestingly, for astronomical systems such as our Sun, the values of large $V\&L$ and small λ results in a very large magnetic Reynolds number, $R_\mathrm{m} \gg 1$. In the ideal MHD limit, where R_m is large, the diffusive term will be negligible as compared to the advective term, and hence, we can ignore the second term of the induction equation. This means that in a highly conductive medium with a high Reynolds number, the magnetic field simply moves with the plasma material without exhibiting significant decay over time, as if the magnetic fields are 'frozen' inside the plasma and it moves with it. This phenomenon is famously referred to as Alfven's theorem of flux freezing (Alfvén, 1942; Alfven, 1950). However, in dynamo theory, diffusion remains critical, particularly at small length scales. Since, the diffusive term scales as L^{-2}, the dynamo will always generate scales at small enough L that the diffusion term becomes comparable to the advection term. This interplay is essential for influencing global dynamo behavior, such as the formation of coherent structures through selective dissipation of energy over magnetic helicity. For a detailed explanation of this theorem or an elaborative mathematical discussion of MHD and dynamos, please refer to Choudhuri (1998)."

Now, there can be two approaches to move further and solve the induction equation and

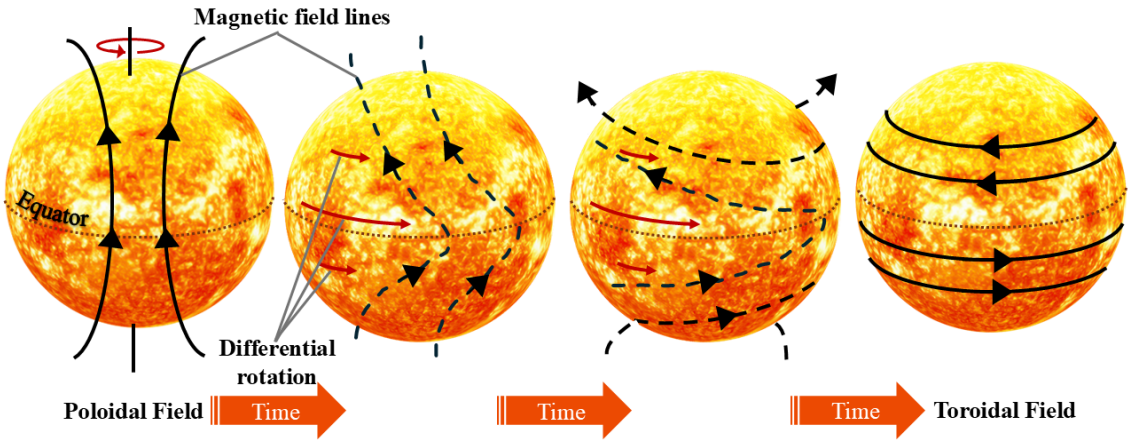

Figure 1.16: Pictorial illustration of the Ω effect

to reproduce the regular features of solar magnetism. One is the kinematic approach, and the other one is the non-kinematic approach. Thus, in the former approach, the induction equation alone is sufficient to understand the evolution of the magnetic field by specifying the velocity field. At first glance, this assumption may seem arbitrary; however, recent observations of solar differential rotation and meridional circulation (Christensen-Dalsgaard, 2002) have demonstrated that this assumption is quite reasonable. Let us discuss this kinematic model in more detail.

1.3.2 Kinematic mean-field dynamo model

It was Eugene Parker, who significantly revolutionized the solar dynamo theory. He suggested that the poloidal field of the Sun is sustained by the turbulent motion of inherently non-axisymmetric ionized plasma in CZ (Parker, 1955a). According to his theory, the poloidal field is stretched in the azimuthal (ϕ) direction due to shear created by differential rotation, facilitated by the flux freezing phenomenon, and forms the toroidal field. This induced shear in the convection zone generates a strong toroidal field in the form of flux tubes–bundles of concentrated magnetic field lines. This phenomenon (as illustrated in Fig. 1.16) of stretching out the poloidal field in the toroidal direction is popularly known as the Ω effect. Even with the magnetic and velocity fields considered as axisymmetric and large-scale differential rotation and meridional circulation included, we would not obtain a self-sustained large-scale magnetic dynamo. This issue, known as Cowling's

anti-dynamo theorem, was first identified by Cowling (Cowling, 1933). Parker (Parker, 1955b) later resolved this by proposing that helical turbulent flows on toroidal flux loops act as a source term for generating the poloidal field.

Parker further introduced the concept of magnetic buoyancy (Parker, 1955b), which explains the formation of bipolar sunspots on the solar surface. As magnetic flux tubes rise through the convection zone, they experience a buoyant force due to their lower density compared to the surrounding plasma. This buoyancy allows the tubes to ascend, carrying their magnetic field with them.

Since the convection zone itself is markedly turbulent, characterized by intense plasma flows and the continuous rise of hot plasma and descent of cooler plasma. Parker proposed that the hot uprising plasma blobs, carrying the toroidal field, are influenced by the Coriolis force due to the Sun's rotation, causing these plasma blobs to twist while moving upward. This twisting alters the magnetic fields, adding a significant poloidal component. The diffusion of these numerous twisted, turbulent eddies gradually reforms the Sun's poloidal field. Given that the Coriolis force operates in reverse directions in the two hemispheres, and the toroidal field also reverses, these dynamics facilitate the formation of a large-scale poloidal field that resembles the structure of a bar magnet with opposite polarities at each pole. This phenomenon of generation of a poloidal field from a toroidal one is known as the α effect. I refer the reader to Fig. 1.17 for pictorial representation of α effect.

Following Parker's proposal, Steenbeck et al. (1966) created a comprehensive mathematical framework for his turbulent dynamo theory. To tackle turbulence in the convection zone, Steenbeck & Krause (1969) adopted an ensemble approach to analyze statistical properties, leading to the development of mean-field dynamo theory. Since the length and time scales of the Sun's large-scale magnetic field are significantly greater than those of the turbulent eddies, in this theory, both the velocity and magnetic fields are represented as the combination of the large-scale mean and small-scale fluctuating components within the turbulent system, which can be expressed as:

$$\mathbf{V} = \langle \mathbf{V} \rangle + \mathbf{V}', \ \mathbf{B} = \langle \mathbf{B} \rangle + \mathbf{B}', \tag{1.5}$$

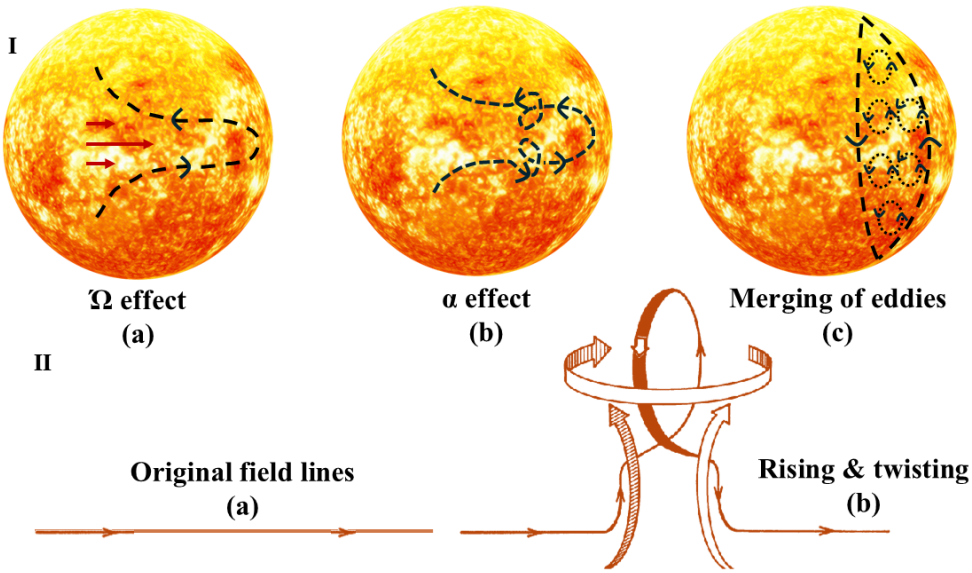

Figure 1.17: Pictorial illustration of the α effect: (I) (a) Ω effect (refer Fig. 1.16 for generation of the toroidal field) (b) Rising and twisting of field lines (refer to II for a clearer view) (c) Generation of the poloidal field through the merging the eddies (Inspired by (Choudhuri, 1998)).

Let us now substitute Eq. (1.5) in Eq. (1.4), and recollecting $\langle \mathrm{B}' \rangle = \langle \mathrm{V}' \rangle = 0$, we get the induction equation in the following form;

$$\frac{\partial \langle \mathbf{B} \rangle}{\partial t} = \nabla \times (\langle \mathbf{V} \rangle \times \langle \mathbf{B} \rangle) + \nabla \times (\langle \mathbf{V}' \times \mathbf{B}' \rangle) - \nabla \times (\lambda \nabla \times \langle \mathbf{B} \rangle) \tag{1.6}$$

Since the equation contains only average values, we shall now denote these average quantities without using angular brackets in the following way;

$$\frac{\partial \mathbf{B}}{\partial t} = \nabla \times (\mathbf{V} \times \mathbf{B}) + \nabla \times \boldsymbol{\varepsilon} - \nabla \times (\lambda \nabla \times \mathbf{B}) \tag{1.7}$$

Here, $\boldsymbol{\varepsilon} = \langle \mathbf{V}' \times \mathbf{B}' \rangle$, which is the mean-field electromotive force, and for an isotropic and homogeneous medium, we can ignore the higher-order terms, which will give the emf of the following form:

$$\boldsymbol{\varepsilon} = \alpha \mathbf{B} - \eta_t \nabla \times \mathbf{B} \tag{1.8}$$

Here, α and η_t are the alpha coefficient and turbulent diffusivity tensors, respectively. Now, substituting Eq. (1.8) in Eq. (1.7), we get;

$$\frac{\partial \mathbf{B}}{\partial t} = \nabla \times (\mathbf{V} \times \mathbf{B} + \alpha \mathbf{B} - \eta_t \nabla \times \mathbf{B}) \tag{1.9}$$

where, η denotes the total diffusivity, which includes the magnetic and turbulent diffusivity of the plasma system.

This formulation of the induction equation can now be applied directly to dynamo modeling. Generally, there are two main strategies for tackling the equation. The first approach uses an axisymmetric mean-field framework, treating both the velocity and magnetic fields in terms of their average, and solves the resulting equations governing the evolution of toroidal and poloidal components. The second approach uses a three-dimensional model to solve the full induction equation, without relying on axisymmetry assumptions. In this thesis, we have employed both types of models to investigate the magnetic cycle activity in the Sun and Sun-like stars. Below is some information regarding the axisymmetric approach, while the details of the three-dimensional STABLE model will be discussed in Chapters 3 and 4.

Observations of the Sun's large-scale magnetic field—such as the shape of the solar corona, the butterfly diagram of sunspots and magnetic field patterns, and Hale's polarity law—indicate that it is largely axisymmetric around the Sun's rotation axis and exhibits antisymmetry across the equator. Consequently, the Sun's magnetic field and velocity fields can be represented as follows:

$$\mathbf{B}_{\text{total}} = \mathbf{B_p} + \mathbf{B}_\phi = \nabla \times [A(r,\theta,t)\hat{\boldsymbol{\phi}}] + B(r,\theta,t)\hat{\boldsymbol{\phi}}, \tag{1.10}$$

$$\mathbf{V} = v_r\hat{r} + v_\theta\hat{\theta} + v_\phi\hat{\boldsymbol{\phi}} = \mathbf{v_P}(r,\theta) + \Omega r\sin\theta\hat{\boldsymbol{\phi}} \tag{1.11}$$

where $\mathbf{B_p} = \nabla \times [A\hat{\boldsymbol{\phi}}]$ is the poloidal component of the magnetic field and B_ϕ is the toroidal one. $\mathbf{v_P}(r,\theta)$ includes the meridional circulation (v_r, v_θ), and Ω is the angular velocity. Substituting the axisymmetric velocity and magnetic field in the Eq. (1.9) and considering $\alpha\Omega$ dynamo, one can obtain (for complete derivation, see Choudhuri, 1998; Charbonneau, 2010; Priest, 2014),

$$\frac{\partial B}{\partial t} + \frac{1}{r}\left[\frac{\partial}{\partial r}(rv_rB) + \frac{\partial}{\partial\theta}(v_\theta B)\right] = \eta_t\left(\nabla^2 - \frac{1}{s^2}\right)B + s(\mathbf{B_p}\cdot\nabla)\Omega + \frac{1}{r}\frac{d\eta_t}{dr}\frac{\partial}{\partial r}(rB), \tag{1.12}$$

$$\frac{\partial A}{\partial t} + \frac{1}{s}(\mathbf{V}\cdot\nabla)(sA) = \eta_t\left(\nabla^2 - \frac{1}{s^2}\right)A + S(r,\theta;B). \tag{1.13}$$

Eq. (1.12) represents the toroidal field evolution equation, with $s(\mathbf{B_p} \cdot \nabla)\Omega$ serving as the source term. If we keep aside the turbulent diffusion and transport terms and focus solely on the source term, then this shear term (source term) is responsible for amplifying the poloidal field ($\mathbf{B_p} = \nabla \times [A\hat{\phi}]$) in proportion to the gradient of the differential rotation, as illustrated in Fig. 1.16. On the other hand, Eq. (1.13) is the poloidal field evolution equation, which includes the diffusion term ($\eta_t \left(\nabla^2 - \frac{1}{s^2}\right) A$), and the transport term ($\frac{1}{s}(\mathbf{V} \cdot \nabla)(sA)$) respectively. The source term in this equation is represented by $S(r, \theta; B)$. There are two primary mechanisms for the generation of the poloidal field: the α effect and the Babcock–Leighton α effect. The details of these two processes, along with the important parameters required to solve the dynamo equations, are explained in the next section.

Crucial parameters in dynamo model

(a) Turbulent diffusivity:

Diffusivity is a crucial component in dynamo models, as it enables the magnetic field to diffuse through the convection zone, counterbalancing the magnetic field generation by the dynamo. This diffusion is essential for understanding how magnetic fields evolve and dissipate over time. The strength of turbulent diffusivity directly affects the timescale of the solar/stellar cycle. Higher turbulent diffusivity results in faster magnetic field diffusion, shortening the cycle period, whereas lower diffusivity slows down the dynamo process. Magnetic diffusivity also plays a role in explaining the decay of sunspots and the dissipation of magnetic flux in active regions. Moreover, turbulent diffusivity is key to reconciling large-scale solar magnetic field dynamics with observed phenomena, such as the polarity reversal during the solar cycle. It also regulates the extent to which the star's magnetic field penetrates deeper into the interior or rises toward the surface, helping to explain phenomena like the migration of starspots.

Their profiles shall be specified separately in each corresponding work.

In all the works referenced in this thesis, we have ignored the variation of diffusivity

with the rotation rate and magnetic field due to the limited knowledge regarding its estimation in different stars.

(b) Meridional velocity:

Meridional circulation is a key ingredient in dynamo theory. While it has been well measured and observed on the solar surface using various techniques, the equatorward return flow still lacks strong observational support. Nevertheless, by applying the principle of mass conservation, it is possible to construct a reasonable profile of meridional circulation based on its observed surface values. In solar dynamo models, meridional circulation is typically considered as a single-cell flow: poleward near the surface and equatorward at the base of the convection zone (CZ). The one-cell per hemisphere meridional flow predicted by the model for the sun agrees with the recent seismological detection (Rajaguru & Antia, 2015; Gizon et al., 2020)

Due to the lack of detailed knowledge about meridional flow in other Sun-like stars, we use the profiles developed by Kitchatinov & Olemskoy (2011b, 2012c). They model the large-scale flows based on the mean-field hydrodynamics model (Ruediger, 1989), which jointly computes differential rotation, meridional flow, and heat transport in the stellar convection zone.

(c) Differential rotation:

Differential rotation is a critical driver of magnetic field generation and is a well established concept ubiquitous in models, theories, and observations. Several models have been developed to parameterize this process (Barnes et al., 2005; Viviani et al., 2019a; Käpylä et al., 2023). In this thesis, differential rotation comes from the model of profiles developed by Kitchatinov & Olemskoy (2011b, 2012c). This numerical model jointly solves the mean-field equations for the angular velocity, meridional flow, and heat transport in a spherical layer of a stellar convection zone. The model produces the solar-type differential rotation as a consequence of angular momentum fluxes. The computed dependence of differential rotation on stellar rotation rate and spectral type (Kitchatinov & Olemskoy, 2012c) is in at least qualitative agreement

with observations by Barnes et al. (2005) and Balona & Abedigamba (2016).

(d) Helical turbulence (α effect): A hint about poloidal field generation:

Parker (1955a) introduced the key idea of poloidal field regeneration. According to his theory, in the highly turbulent solar convection zone, the toroidal field is lifted due to magnetic buoyancy. As this rising plasma interacts with the Coriolis force, it undergoes a helical twist. According to Alfvén's flux-freezing principle, the magnetic field lines remain embedded in the plasma and are twisted by this helical turbulence. This process occurs in a rotating frame of reference, creating vorticity in opposite directions in the two hemispheres. Consequently, the toroidal magnetic field twists in opposite directions in each hemisphere. This results in magnetic loops in the poloidal plane exhibiting the same orientation in both hemispheres (as seen in Fig. 1.17). The strong turbulent diffusion within the convection zone causes these numerous loops to form a large-scale poloidal magnetic field collectively. This mechanism, known as the turbulent α effect, allows the generation of the poloidal field from the toroidal field through helical turbulence.

The solar dynamo is sustained by the continuous generation of the toroidal field from the poloidal field through differential rotation (the Ω effect) and the regeneration of the poloidal field from the toroidal field via the α effect. This interplay between the two effects explains the Sun's magnetic cycle and its long-term persistence.

However, it was later realized that in the presence of a strong toroidal magnetic field (10^5 G), the turbulent α effect in the convection zone would struggle to regenerate the poloidal field through helical turbulence alone (Choudhuri & Gilman, 1987; D'Silva & Choudhuri, 1993). To address this, researchers adopted the Babcock–Leighton α effect, whose detailed discussion is done in the next section.

1.3.3 Babcock-Leighton process and Flux transport dynamo

Although the mean-field turbulent dynamo theory explained many features of solar magnetism and provided important insights into solar activity, by the late 20th century, new

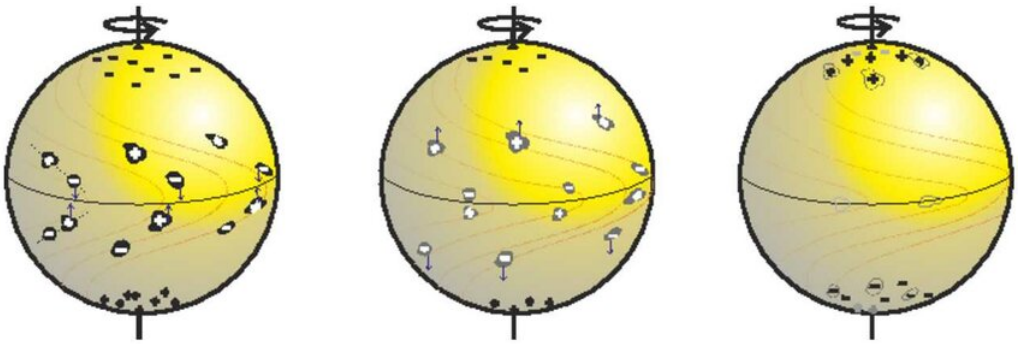

Figure 1.18: Pictorial illustration of the Babcock–Leighton process: The BMR deposit of the surface (leftmost image) decays and is dispersed (middle image) and forms the poloidal field of the opposite polarity (rightmost). Image credit: (Charbonneau & Sokoloff, 2023).

observations and simulations suggested that it might not fully explain the complexities of the solar dynamo. The traditional α effect proposes that the helical convective turbulence in the convection zone twists the toroidal field, thereby generating a poloidal component. However, this twisting can occur only if the energy density of the toroidal magnetic field is lower than that of the convective turbulence. Thin flux tube simulations (D'Silva & Choudhuri, 1993; Fan et al., 1994) indicate that the magnetic field throughout the convection zone can reach strengths of the order of 10^5 G. Under these conditions, the convective motions are too weak to effectively twist the intense toroidal field. Consequently, the α effect alone cannot adequately explain the generation of the poloidal field.

The strong observational evidence later combined with the theoretical limitations mentioned above, led researcher to explore other mechanisms that could better account for the generation of the poloidal field and match with the observations. Hence, Babcock–Leighton mechanism came into the picture.

It was introduced by Babcock (1961) and later refined by Leighton (1964, 1969), hence the name Babcock–Leighton. This process has been confirmed by synoptic magnetograms (Mordvinov et al., 2020, 2022) and well-reproduced in Surface Flux Transport (SFT) models (Wang et al., 1989; Dasi-Espuig et al., 2010; Kitchatinov & Olemskoy, 2011b; Upton & Hathaway, 2014; Jiang et al., 2014b; Lemerle et al., 2015). According to the Babcock–Leighton process, the poloidal field is generated through the decay and dispersal of tilted active regions (sunspots or bipolar magnetic regions (BMRs)) near the solar surface. The

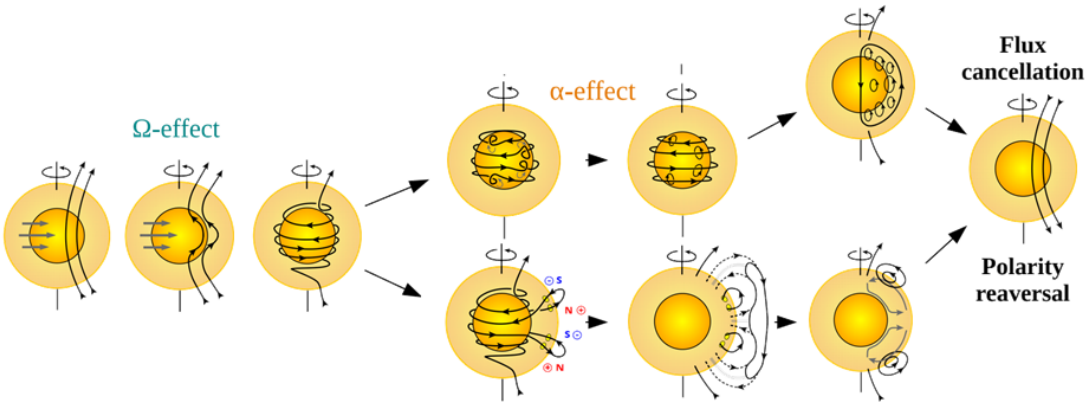

Figure 1.19: Pictorial representation of the solar/stellar dynamo theory. Image credit: Noraz et al. (2022a)

BMRs are tilted relative to the equator, meaning that the leading and trailing magnetic polarities are not aligned at the same latitude. Typically, the leading polarity forms closer to the equator, while the trailing polarity appears at a slightly higher latitude, following Joy's law (Hale et al., 1919). This latitudinal difference causes the two polarities to evolve differently as they interact with surrounding plasma flows. Due to this tilt, the leading spots (which are closer to the equator) often cross into the opposite hemisphere, where they cancel out with spots of the opposite polarity, a process commonly referred to as cross-equatorial cancellation. Meanwhile, the trailing spots (located at higher latitudes) are carried toward the poles, where they neutralize the polar field from the previous cycle and help build the polar field for the next cycle.

This mechanism does not need to be extremely efficient to have a significant impact because the total magnetic flux of the peak polar field in the polar region is comparable to the flux contained within just one BMR, which is approximately 10^{22} Mx. Many recent dynamo models incorporate the Babcock–Leighton mechanism and are referred to as Babcock–Leighton type flux transport dynamo models. In addition to Surface Flux Transport (SFT) models and 2D axisymmetric kinematic dynamo models, the B-L process has also been successfully captured in 3D dynamo models (Yeates & Muñoz-Jaramillo, 2013; Miesch & Dikpati, 2014).

The complete dynamo process is summarized in Figs. 1.19 and 1.20, and the summary of

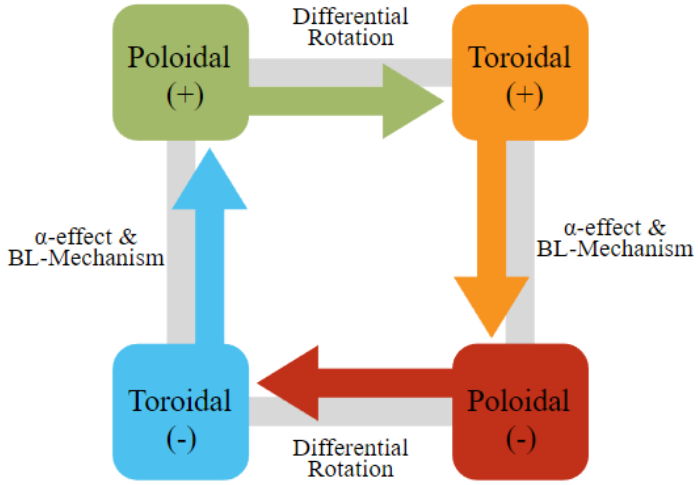

Figure 1.20: Cyclic representataion of the solar/stellar dynamo theory

the Babcock-Leighton type dynamo models is as follows:

During a solar minimum, the poloidal field reaches its peak strength, which is then gradually converted into the toroidal field by the solar differential rotation. Sunspots are then form from toroidal flux tubes, and solar activity increases as the cycle progresses. The equatorward meridional flow transports the toroidal field towards the equator, causing sunspots to appear closer to the equator over time. At solar maximum, the poloidal field weakens, and its polarity reverses, while the solar magnetic field becomes dominated by the toroidal component. This generation of the toroidal field from the poloidal field is a linear and predictable process.

Once sunspots, or BMRs, emerge on the solar surface, they decay over time due to diffusion and cancellation of magnetic flux between opposite polarities. The tilt of the BMRs causes the remnant magnetic field at higher latitudes to be carried toward the poles by the poleward meridional flow and diffusion. This process, where the poloidal field is regenerated from the decay of sunspots, forms the core of the Babcock–Leighton mechanism. However, the stochastic nature of BMR properties—such as their tilt, magnetic flux, and rate of emergence—introduces variability in the contribution of each BMR to the polar field. This makes long-term, multi-cycle solar activity forecasts challenging and less predictable.

Despite several challenges, Babcock–Leighton-type dynamo models and SFT simulations have successfully reproduced most of the observed features of the solar cycles and are currently the most widely accepted theory for the solar dynamo (Charbonneau, 2010, 2020; Karak, 2023a; Cameron & Schüssler, 2023).

1.3.4 Babcock-Leighton mechanism in Sun-like stars

Similar to the sun, other sun-like stars also have convection zones in their outer layers; hence, it is natural to expect that these stars also support dynamo action, which maintains the stellar magnetic cycles.

In the Babcock-Leighton process for sun, tilted bipolar magnetic regions decay and disperse to produce a poloidal field through turbulent diffusion, meridional flow, and differential rotation. Therefore, the key ingredients in the Babcock–Leighton process are the tilt and the latitudinal position of BMR emergence. In fact, many theories show that the higher the latitude, the less effective the poloidal field generation is (Muñoz-Jaramillo et al., 2013; Cameron & Schüssler, 2015; Jiang et al., 2014b). This phenomenon is a key to well-known latitudinal quenching (Petrovay, 2020; Jiang, 2020; Karak, 2020), implying that stronger cycles that produce sunspots at higher latitudes are less effective in generating a poloidal field. In short, tilt and latitude play a crucial role in the effectiveness of the Babcock–Leighton process.

As the star spots are believed to be produced through the rise of the toroidal flux tubes from the deeper convection zone and during the rise of flux tubes, the Coriolis force acting on the diverging flows arising from the apex of the tubes, the tilt and the emerging latitudes are expected to increase with the increase of rotation rates of stars (Işık et al., 2018). In fact, many studies suggest that young-rapidly rotating sun-like stars show star spot appear at high latitudes (Schuessler & Solanki, 1992a; Schuessler et al., 1996; Luo et al., 2022). Thus, the natural question arises: does the BL process operate in rapidly rotating stars? We shall address this question in Chapter 5.

On the other end of the rotation range are stars rotating more slowly than the Sun. Some

simulations have observed a transition from solar-like to anti-solar differential rotation in these stars (Gilman, 1977; Guerrero et al., 2013; Gastine et al., 2014; Käpylä et al., 2014; Fan & Fang, 2014; Karak et al., 2015a; Featherstone & Miesch, 2015; Karak et al., 2018b). However, the question remains as to whether magnetic field reversals occur in this regime. Therefore, we shall investigate the operation of the Babcock–Leighton process in slowly rotating stars in Chapter 7.

In this thesis, I have undertaken a detailed and comprehensive effort to reproduce key stellar features by employing various dynamo models. I aim to capture the complex dynamics of stellar magnetic cycles, including the relationships between rotation rate, cycle period, magnetic activity, and long-term variability. By exploring different configurations and modifications of dynamo models— I also aim to provide a deeper understanding of how these models can account for observed stellar phenomena while also addressing their current limitations.

1.4 Outline of the Thesis

The rest of my thesis is organized into six chapters, each focusing on unique aspects of solar and stellar magnetic activity, with a special emphasis on understanding how magnetic cycles operate in stars using different dynamo models, particularly the Babcock-Leighton process. Chapter 2 introduces the basics of magnetic field generation in Sun-like stars and explores the possible operation of a dynamo below the critical dynamo number. Chapter 3 examines how large- and small-scale dynamos coexist in stars and investigates hysteresis, where different dynamo solutions arise depending on initial conditions. Chapter 4 looks at the role of meridional circulation in magnetic field generation, how changes in flow speed impact the strength and duration of magnetic cycles, and the connection to a star's rotation rate. Chapter 5 focuses on the operation of the Babcock–Leighton dynamo in rapidly rotating stars. In rapidly rotating stars, BMRs are expected to emerge at high latitudes, which are less efficient in generating the poloidal field due to poor cross-equatorial cancellation. Therefore, the operation of the Babcock-Leighton dynamo in rapidly rotating stars is questionable. Therefore, using a 3D kinematic dynamo model, STABLE, I shall explore

this question. In Chapter 6, I discuss how differential rotation, in addition to meridional flow within the star's convection zone, plays a crucial role in dynamo operation. We also study how rapidly rotating stars exhibit more irregular and stronger magnetic activity than slower rotating stars, with fewer occurrences of grand minima, where magnetic activity significantly drops. Transitioning from this, I then address slowly rotating stars, which rotate slower than the Sun, in Chapter 7. Here, I will explore the possible operation of a dynamo in stars that rotate ever slower than the Sun and exhibit anti-solar differential rotation. Through these studies, we provide insights into the strengths and limitations of current dynamo models and how they apply to stars with different rotation periods. Finally, in Chapter 8, the key findings of the thesis are summarized.